THE JOURNAL OF PHYSICAL CHEMISTRY A

Article

pubs.acs.org/JPCA

Piezoelectric Hydrogen Bonding: Computational Screening for a Design Rationale

Keith A. Werling, Maryanne Griffin, Geoffrey R. Hutchison, and Daniel S. Lambrecht*

Department of Chemistry, University of Pittsburgh, 219 Parkman Avenue, Pittsburgh, Pennsylvania 15260, United States

Supporting Information

ABSTRACT: Organic piezoelectric materials are promising targets in applications such as energy harvesting or mechanical sensors and actuators. In a recent paper (Werling, K. A.; et al. *J. Phys. Chem. Lett.* **2013**, *4*, 1365−1370), we have shown that hydrogen bonding gives rise to a significant piezoelectric response. In this article, we aim to find organic hydrogen bonded systems with increased piezo-response by investigating different hydrogen bonding motifs and by tailoring the hydrogen bond strength via functionalization. The largest piezo-coefficient of 23 pm/V is found for the nitrobenzene−aniline dimer. We develop a simple, yet surprisingly accurate rationale to predict piezo-coefficients based on the zero-field compliance matrix and dipole derivatives. This rationale increases the speed of first-principles piezo-coefficient calculations by an order of magnitude. At the same time, it suggests how to understand and further increase the piezo-response. Our rationale also explains the remarkably large piezo-response of 150 pm/V and more for another class of systems, the "molecular springs" (Marvin, C.; et al. *J. Phys. Chem. C* **2013**, *117*, 16783−16790.).

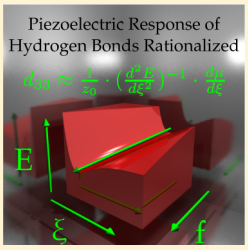

INTRODUCTION

Energy harvesting, or the conversion of ambient background energy, typically in mechanical or thermal forms, into useful electrical resources has gained increasing interest for improving the energy efficiency of devices as well as a resource in its own right. For example, piezoelectric materials interconvert motion and force into electrical currents (cf., ref 3 for a review and refs 4−8 for examples of computational screening approaches for inorganic piezoelectric materials). While most highly responsive piezomaterials are ceramics or semicrystalline polymers such as poly vinylidene difluoride (PVDF),[9] designed flexible organic solids remain an attractive target for energy harvesting.

While the general prediction of molecular crystal structures is an active area of research, crystal design and engineering of small-molecule compounds to form self-assembled polar organic crystals, for example, *m*-nitroaniline,[10,11] 2-methyl-4-nitroaniline,[12,13] or 3-furyl methacrylic anhydride,[14] have led to the discovery of highly polar materials, including nonlinear optical materials and piezoelectrics.

In a recent publication, we demonstrated that organic hydrogen-bonded materials give rise to significant piezoelectricity.[1] An electromechanically responsive hydrogen bond is interesting from both a materials design and a chemistry perspective. Hydrogen bonds are ubiquitous in chemistry and biology and have been frequently used to drive self-assembly in polar organic materials.[15−20] Consequently, piezo-response should be ubiquitous in molecular materials[1,2,21] and suggests that the detailed electromechanical response of hydrogen bonds should be investigated further.

In this work, we consider the basic deformation of a series of hydrogen-bonded dimers under an applied electric field using first-principles quantum chemical methods. We find both small and large electromechanical deformations dependent on the force constant of the hydrogen bonding interaction and the electrostatic charges involved in the hydrogen bonds. This leads to a simplified design criterion to find highly responsive interactions.

RATIONAL EXPLANATION OF PIEZOELECTRICITY

The practical calculation of piezo-coefficients for molecular systems is rather straightforward and is outlined, for example, in our earlier publication.[1,2] Basically, one simply calculates the equilibrium bond lengths or molecular dimensions after geometry optimization at varying applied electric fields. Within the linear regime, a plot of the length (bond or molecule) versus field strength and its linear regression yield the piezo-coefficient. For a general outline of the theory of piezoelectricity, we refer the reader to ref 21. In this section we address the question: What are the intrinsic molecular properties that give rise to piezoelectricity, as opposed to bulk properties, and how can one *rationalize* the different piezo-coefficients of different systems?

A schematic diagram of a simple system that possesses an energy surface similar to our hydrogen bonded systems is depicted in Figure 1. One can derive a compellingly simple estimate for the piezo-coefficient. On the basis of considerations of how much the equilibrium bond length of the piezoelectric bond changes upon application of an external field, and using a Taylor expansion of the potential energy surface along the direction under consideration, z, and the field strength f, the piezo-coefficient can be estimated as

Special Issue: Kenneth D. Jordan Festschrift

Received: December 29, 2013
Revised: February 26, 2014
Published: February 28, 2014

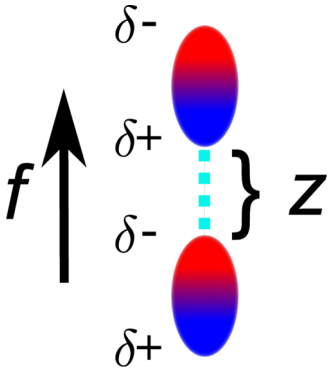

Figure 1. Generic system of two polar monomers separated by distance z and subject to electric field f along the z direction. z corresponds to the hydrogen bond length in the systems we studied here.

$$d_{33} \approx \frac{1}{z_0} \cdot \frac{\partial^2 E}{\partial \xi^2}\bigg|_{(z_0,0)} \frac{\partial \mu}{\partial \xi}\bigg|_{(z_0,0)} \equiv -\frac{1}{z_0} h_{0\xi\xi}{}^{-1} \mu_{0\xi} \quad (1)$$

Here, z_0 is the equilibrium bond length, $E(\xi,f)$ the energy as a function of geometry displacement ξ (i.e., $z - z_0$) from the equilibrium, and f the electric field strength. Note that the derivatives are evaluated for the equilibrium structure at zero field (i.e., $(z, f) = (z_0, 0)$). μ is the dipole moment of the system. In our notation, we choose h to represent second derivatives of the energy of the system. The nonzero indexes indicate the variables with respect to which we are differentiating, and the index 0 indicates that the term is evaluated at $(z, f) = (z_0, 0)$. The notation is analogous for first derivatives. Here, we assume that the electromechanical response happens solely along one bond direction, z, and that the electric field is applied along this direction (see Figure 1). A more general derivation of eq 1 as well as some higher-order generalizations are presented in the following section. We note that a relationship between the piezo-coefficient and dipole moment derivative has been discussed earlier,[2] and subsequent to our derivation, we noted that the program package GULP uses a similar expression for estimating the piezoelectric strain/stress constants.[22,23]

In the second line of eq 1 we have introduced a shorthand notation to make the expression more intuitive. As eq 1 suggests, the piezo-coefficient arises, to leading order, from a balance between two factors: the inverse Hessian $h_{0\xi\xi}{}^{-1}$ (or compliance matrix) of the bond and the derivative of the dipole moment with respect to geometric displacements, both evaluated at the equilibrium geometry for zero field along the piezo-active coordinate. This leads to a compellingly simple rationale: To achieve a large piezo-coefficient, one needs to tune the system to have a large compliance (weak bond) for the piezo-response and a large change in dipole moment as the bond length changes.

Is it possible to maximize the two dominating factors, compliance and dipole moment derivative, simultaneously? There are some limiting cases that suggest compliance and dipole moment are in many cases antagonists. For example, consider a pair of bare counterions such as Na^+ and Cl^-. Here, the change in dipole moment with geometric displacement is very large, but the compliance is small because of the strong ionic bond. At the other extreme, consider two helium atoms bound only by van der Waals (vdW) forces. Here the compliance is very large, but the dipole moment as well as its derivative is zero. Both extremes lead to small piezocoefficients. From this, one expects that the optimization of the piezo-coefficient involves, at least for hydrogen-bonded systems, finding a delicate balance between (weak) bonding and (large) dipole moment derivatives.

DERIVATION OF THE THEORETICAL RATIONALE FOR THE PIEZO-COEFFICIENT

The energy surface of our system is a function of monomer distance (z) and external field (f). An illustrative energy contour surface is depicted in Figure 2 and will be referenced during the derivation.

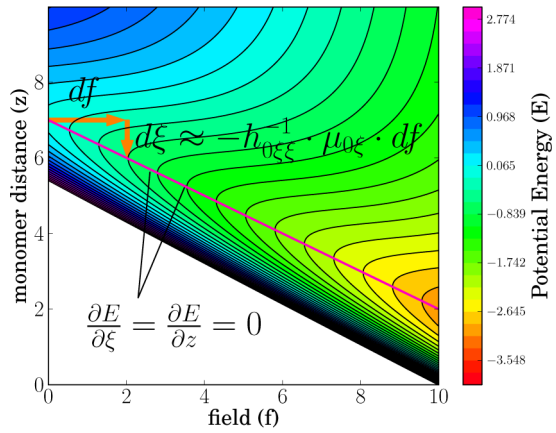

Figure 2. Schematic contour plot of a potential energy surface as a function of monomer separation z and field strength f for a hydrogen -bonded system (all in arbitrary units). The energy minimum for a given field is tracked with the pink solid line along the surface.

Given our equilibrium geometry at zero field (denoted by $(z_0, 0)$), we can approximate the value of z that the system will adopt, when a field is applied, via a Taylor expansion. For convenience we can define a displacement variable $\xi = z - z_0$ (that is the displacement from the equilibrium geometry at zero field) and recognize that all derivatives with respect to ξ are equivalent to derivatives with respect to z. Up to second order in ξ and f the Taylor expansion becomes

$$E(z,f) \approx E(z_0,0) + \frac{\partial E}{\partial \xi}\bigg|_{(z_0,0)} \xi + \frac{\partial E}{\partial f}\bigg|_{(z_0,0)} f + \frac{1}{2}\frac{\partial^2 E}{\partial \xi^2}\bigg|_{(z_0,0)} \xi^2 + \frac{1}{2}\frac{\partial^2 E}{\partial f^2}\bigg|_{(z_0,0)} f^2 + \frac{\partial^2 E}{\partial \xi \partial f}\bigg|_{(z_0,0)} f\xi \quad (2)$$

For convenience we rename all first-order derivatives with g_0 and all second-order derivatives with h_0. We include indexes that suggest the variables with respect to which we are differentiating. The index 0 implies that the derivatives are evaluated at $(z, f) = (z_0,0)$:

$$E(z,f) \approx E(z_0,0) + g_{0\xi}\xi + g_{0f} f + \frac{1}{2} h_{0\xi\xi}\xi^2 + \frac{1}{2} h_{0ff} f^2 + h_{0\xi f} f\xi \quad (3)$$

dx.doi.org/10.1021/jp412740j | J. Phys. Chem. A 2014, 118, 7404−7410

Particularly, we are interested in solving for the displacement, ξ, at a given field strength for which the energy, E, is a minimum, i.e., $(\partial/\partial\xi)E(f) = 0$. This is the analytical equivalent of finding the displacement for the minimum energy geometry as a function of field strength, just as we have done via curve fitting in this work (see computational details section and Supporting Information) and our previous work.[1,2] Referring to Figure 2, the equilibrium bond length as a function of the field strength is tracked via the pink line. We can take the necessary derivatives of the right-hand side of eq 3, set them equal to zero, and solve for ξ as a function of f:

$$g_{0\xi} + h_{0\xi\xi}\xi + h_{0\xi f}f = h_{0\xi\xi}\xi + h_{0\xi f}f = 0 \tag{4}$$

$$\xi(f) = -{h_{0\xi\xi}}^{-1}h_{0\xi f}f \tag{5}$$

where we have used $g_{0\xi} = 0$ because we start from a converged geometry.

Taking the derivative of ξ with respect to the field strength f is analogous to finding the slope of the hydrogen bond length versus field plots (see Supporting Information). Dividing the derivative by the equilibrium distance z_0 then yields the piezo-coefficient up to first order in f:

$$\frac{\mathrm{d}\xi}{\mathrm{d}f} \approx -{h_{0\xi\xi}}^{-1}h_{0\xi f} \tag{6}$$

$$d_{33} \approx -\frac{1}{z_0}{h_{0\xi\xi}}^{-1}h_{0\xi f} \tag{7}$$

We recognize that $h_{0\xi f} \equiv (\partial^2 E/\partial\xi\partial f)|_{(z_0,0)}$ is just the derivative of the dipole of the system with respect to ξ for the optimized starting structure, $\mu_{0\xi} \equiv (\partial\mu/\partial\xi)|_{(z_0,0)}$. Thus, the piezo-coefficient is approximately

$$d_{33} \approx -\frac{1}{z_0}{h_{0\xi\xi}}^{-1}\mu_{0\xi} \tag{8}$$

which concludes the derivation of eq 1.

It is worthwhile at this point to note that eq 6 can also be obtained in a more concise manner. Here we consider the cyclic rule of multivariable calculus. Our variables will be g, ξ, and f, which, as above, are the energy gradient, displacement from equilibrium, and field, respectively. From the cyclic rule, we know

$$\frac{\partial\xi}{\partial f_g}\frac{\partial g}{\partial\xi_f}\frac{\partial f}{\partial g_\xi} = -1 \tag{9}$$

where the subscripts here indicate a variable that is held constant in the corresponding partial derivative. Rearranging the equation, we find

$$\frac{\partial\xi}{\partial f_g} = -\left(\frac{\partial g}{\partial\xi_f}\right)^{-1}\left(\frac{\partial f}{\partial g_\xi}\right)^{-1} \tag{10}$$

and we can note that

$$\left(\frac{\partial f}{\partial g_\xi}\right)^{-1} = \frac{\partial g}{\partial f_\xi} \tag{11}$$

by standard rules of calculus and

$$g = \frac{\partial E}{\partial\xi} \tag{12}$$

Making the appropriate substitutions and dropping our subscript notation except for the term on the left, we obtain:

$$\frac{\partial\xi}{\partial f_g} = -\left(\frac{\partial^2 E}{\partial\xi^2}\right)^{-1}\frac{\partial^2 E}{\partial\xi\partial f} \tag{13}$$

This is essentially the same result as eq 6, where the left-hand side is now a partial derivative. However, in this second derivation the result holds for any point on the potential energy surface, i.e., the partial derivative can be evaluated for any given separation, field strength, and gradient. In our previous derivation, we assumed that the Taylor expansion is performed around zero for all these variables. In particular, our first derivation imposes the condition of a zero gradient, $g_0 = 0$ when solving for $\xi(f)$. This second derivation gives an alternative that could perhaps be more generally applicable. It is also reassuring that it is possible to rederive eq 6 in this concise, independent way.

In a similar manner to the first derivation, the estimate for the piezo-coefficient can be generalized to second order in the electric field strength f:

$$\begin{aligned}\frac{\mathrm{d}\xi}{\mathrm{d}f} \approx &-\left(\frac{\partial^3 E}{\partial\xi^2\partial f}f + \frac{\partial^2 E}{\partial\xi^2}\right)^{-1}\left(\frac{\partial^2 E}{\partial\xi\partial f} + \frac{\partial^3 E}{\partial\xi\partial f^2}f\right)\\ &+\left(\frac{\partial^3 E}{\partial\xi^2\partial f}f + \frac{\partial^2 E}{\partial\xi^2}\right)^{-2}\left(\frac{\partial^2 E}{\partial\xi\partial f}f + \frac{1}{2}\frac{\partial^3 E}{\partial\xi\partial f^2}f^2\right)\frac{\partial^3 E}{\partial\xi^2\partial f}\end{aligned} \tag{14}$$

For brevity we drop the $|_{(z_0,0)}$ notation for the derivatives and understand that they are evaluated at $(z_0, 0)$ as before. We note that this expression simplifies to eq 1 when one lets $f \to 0$. Equation 14 extends the previously described estimate for the piezo-coefficient to include deviations from the linear regime in the piezo-response, which could potentially be relevant for large field strengths and/or strong piezo-responses. Recasting in terms of the gradient and Hessian with respect to nuclear displacements as well as the dipole moment and polarizability $\alpha \equiv (\partial^2 E/\partial f^2)|_{(z_0,0)}$, eq 14 takes on the more compact form:

$$\begin{aligned}\frac{\mathrm{d}\xi}{\mathrm{d}f} \approx &-\left(\frac{\partial h}{\partial f}f + h\right)^{-1}\left(\frac{\partial\mu}{\partial\xi} + \frac{\partial\alpha}{\partial\xi}f\right) + \left(\frac{\partial h}{\partial f}f + h\right)^{-2}\\ &\left(\frac{\partial\mu}{\partial\xi}f + \frac{1}{2}\frac{\partial\alpha}{\partial\xi}f^2\right)\frac{\partial h}{\partial f}\end{aligned} \tag{15}$$

The first line can be seen to be an extension of eq 1 to include the responses of the Hessian and the dipole moment derivative up to linear order in f.

RESULTS AND DISCUSSION

For a systematic investigation of the correlation between hydrogen bonding and piezo-coefficients, we selected a range of organic hydrogen-bonded systems with varying bond strengths (Figure 3). Motivated by the known[1,12,13] piezoelectricity of the $NO_2\cdots H_2N$ bond, we initially included dimers with single and double bonds of this type. Since the piezo-responses for double bonded systems were rather small (likely due to the expected small compliance of these hydrogen bonds), we concentrate in the following on singly bonded systems.

dx.doi.org/10.1021/jp412740j | J. Phys. Chem. A 2014, 118, 7404−7410

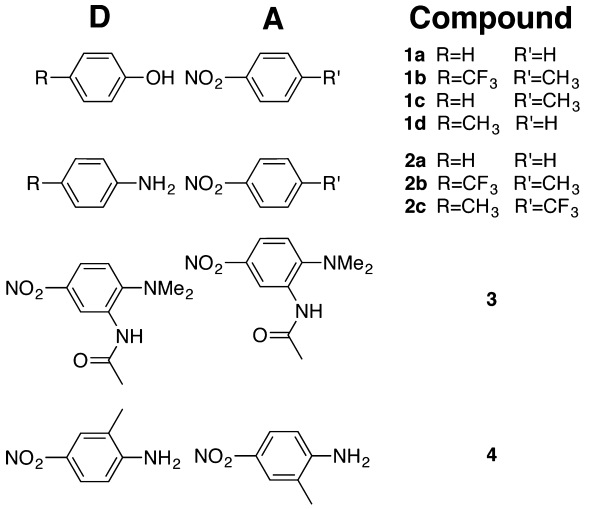

Figure 3. Molecules studied to test piezoelectric deformation of hydrogen bonds.

We expect that the hydrogen bond strength and thus piezoelectricity can be controlled by varying the hydrogen donor/acceptor pair. To test this hypothesis, we include OH···H_2N as well as carbonyl−amid hydrogen bonding motifs. We also expect that the hydrogen bond strength can be tuned by adding electron donating or withdrawing groups to the aromats. For this purpose, we add methyl and trifluoromethyl substituents in para position for the singly bonded systems. Finally, we include *N*-[2-(dimethylamino)-5-nitrophenyl]-acetamide **3** and 2-methyl-4-nitroaniline **4**, due to their known field-dependent polarizability and piezoelectric properties.[1,12,13,24,25] We note that the experimentally measurable piezoelectricity of **3** probably does not arise from hydrogen bonding, but we can still investigate the piezoelectric properties of the hydrogen bond in the dimer for the purpose of analysis.

The piezo-coefficients and hydrogen bond strengths were calculated as outlined in the computational details section, and the dependence of d_{33} on the bond energies is plotted in Figure 4 . For the series of NH_2···O_2N dimers and their derivatives, we find a d_{33} vs bond strength plot that resembles a volcano plot as known from catalysis (cf., ref 26). Initially we believed this could be rationalized by considering the previous discussion of eq 1, where we proposed that in hydrogen-bonded systems a weaker hydrogen bond strength (expected large compliance matrix) is typically connected with a smaller dipole derivative, whereas a bond with large dipole derivative typically has a smaller compliance. Not surprisingly, we might expect this antagonism to lead to a volcano plot. However, our analysis was based on the assumption that low bond strength is indicative of high compliance and that high bond strength is indicative of low compliance. Analysis of our data yields no clear correlation between hydrogen bond strength and curvature. We anticipated for these types of systems that a larger potential well depth (hydrogen bond strength) would also indicate higher curvature (low compliance), but this is not necessarily the case even within this series of rather homologous molecules. For the OH···O_2N dimer, the piezo-coefficient is smaller than for NH_2···O_2N, and their derivatives show a similar volcano plot.

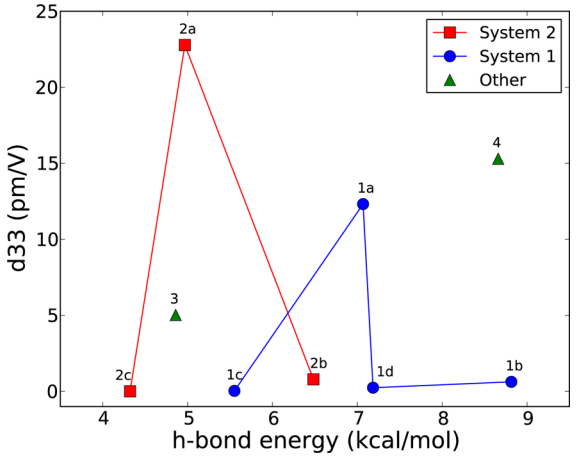

Figure 4. Plot of calculated piezo-coefficients (pm/V) versus calculated hydrogen bond strengths (kcal/mol) for different hydrogen bond types as well as different electron donating and withdrawing groups. Lines are just guides to the eye.

The largest piezo-coefficient of 23 pm/V is found for the aniline−nitrobenzene dimer **1a**, followed by 2-methyl-4-nitroaniline **4** with 15 pm/V, and phenol-nitrobenzene with 12 pm/V **2a**. The trend between **2a** and **1a** can be correlated with the increasing bond strength, although, as previously mentioned, higher bond strength does not necessarily indicate a lower compliance. It is interesting to note that **4** exhibits a piezo-coefficient similar to **1a**, although its hydrogen bond strength is among the largest in the test. For the slightly exotic hydrogen bonded system *N*-[2-(dimethylamino)-5-nitrophenyl]-acetamide **3**, the piezo-coefficient of 5 pm/V is relatively small. Interestingly, the hydrogen bond strength is very similar to that of **1a**, but d_{33} is smaller by a factor of 3. These findings reiterate that bond strength is not a good indicator of piezo-coefficients for these types of systems. Furthermore, we also need to refine our earlier discussion from the theory section: The dipole derivative and compliance for these compounds do not always show a clear antagonistic relationship. There are several factors at work that influence the piezo-response in these compounds, but their relationships with one another are not necessarily straightforward.

Regardless, below we demonstrate that we can accurately calculate piezo-coefficients via eq 1 by employing compliance and dipole moment derivatives as the only independent descriptors. In Figure 5, we show the correlation between the estimate and the fully calculated piezo-coefficient. Although eq 1 holds only to second order in ξ and mixed first order in ξ/f, fitting all data using linear regression yields a nearly perfect correlation (R^2 = 0.997 and slope =1.02) between estimated and calculated piezo-response.

We remark that for **2a** we have omitted data points for stronger field strengths in the linear regression analysis where the deviation from a linear behavior becomes significant (cf., Supporting Information for details). For stronger piezosystems or for larger field strengths, higher-order terms in the piezo-rationale likely need to be taken into account for an accurate estimate, but here we have only considered the piezocoefficient in the linear regime. Currently, we utilize numerical derivatives for the $\mu_{0\xi}$ term, as outlined in the computational details section. For a more accurate determination of stronger piezosystems, caution must be taken to ensure an adequate approximation of this term. Nevertheless, the performance of the rationale in its current implementation is excellent for the systems considered here, which is impressive considering the simplicity of the rationale.

dx.doi.org/10.1021/jp412740j | J. Phys. Chem. A 2014, 118, 7404−7410

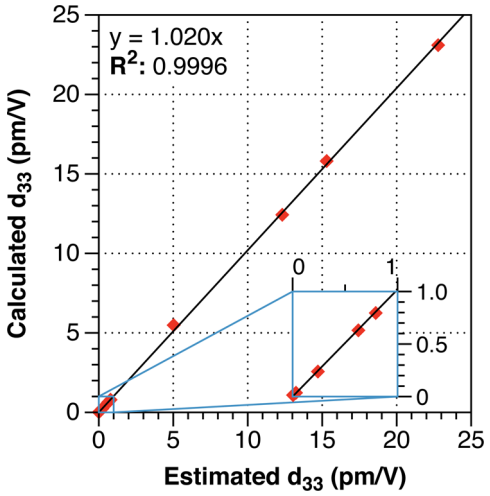

Figure 5. Plot of our estimated piezo-coefficient (eq 1) versus the calculated piezo-coefficients (all in pm/V) for the full data set and (inset) a subset of weak piezoelectrics.

We conclude that eq 1 is quite helpful at guiding the development of stronger hydrogen-bonded piezo-systems and likely also those of molecular springs.[2] It is much cheaper to calculate than our previous methods since all necessary quantities are calculated at $f = 0$, whereas a full calculation requires calculations at five to ten different field strengths (see computational details). The Hessian and dipole moment derivative can be calculated from a curve fit requiring ~10 single-point calculations at most, as compared to about 100 energy evaluations for the alternate approach using multiple geometry optimizations at varying electric field strengths.

There is of course much room for improvement in both the efficiency and accuracy of our approach for the prediciton of piezo-coefficients. In this study, we exploited a system type (i.e., hydrogen-bonded organic molecules), which usually can be approximated as two rigid bodies (the individual molecules in each dimer pair) interacting by a weak potential. We have shown previously that the individual relaxation of intramolecular bond lengths gives rise to a negligible contribution to the piezo-coefficient in a hydrogen-bonded piezo-system.[1] The system thus allows us to reduce the dimensionality of our systems to just one coordinate, the hydrogen bond distance. This is also why it is cheaper and easier in this case to compute the derivatives (Hessian and dipole moment derivate) via single-point energy calculations rather than via analytical derivative methods since the latter typically do not allow to perform the evaluation of only a subset of degrees of freedom at a reduced cost.

However, a more accurate method applicable to more general types of systems is desirable and would likely be required to calculate the coupled response of the energy to displacements along all degrees of freedom. Future studies will likely yield more accurate and efficient methods able to deal with all systems, which will allow for better screening methods to predict promising candidates for more piezo-responsive materials. We are encouraged by our results that such an approach will indeed be feasible.

■ CONCLUSIONS

To find systems with a large piezo-response, one needs to find a bond or vibrational mode with a large compliance (i.e., low force constant) and a large change in dipole moment as the bond length changes. For hydrogen-bonded systems at least, this requires systems that are neither too weakly bound (i.e., low force constant but also small change in dipole moment) nor too strongly bound (i.e., large change in dipole moment, but large force constant). Our computational screening in this work suggests such systems are rare, but one $NH_2\cdots O_2N$ candidate, the simple aniline-nitrobenzene dimer **1a**, has a larger predicted piezo-response (23 pm/V) than 2-methyl-4-nitroaniline **4** (14 pm/V), the organic crystal with the largest known piezoelectric response, and similar to PVDF, the most widely used piezoelectric polymer.

The accuracy of the estimated piezo-coefficient derived here and the high correlation with explicitly calculated geometric deformations suggest a rapid method to screen a wide range of hydrogen bond motifs and molecular materials. While few piezoelectric organic crystals are known, many more likely exist and can be found by high-throughput computational techniques. We anticipate that by subtle tailoring of the substituents with the aniline−nitrobenzene and phenol−nitrobenzene dimers and similar hydrogen-bonded families, we may find larger electromechanical deformations than previously experimentally reported.

Another promising application of the estimate is that it provides a simple rationale for the piezo-response that makes it fairly simple to understand how to obtain increased piezo-coefficients. For example, it can be understood why molecular springs with polar end groups[2] exhibit large piezo-coefficients in excess of 100 pm/V: the restoring force of the spring counteracts the attractive force between the polar end groups, which effectively increases the compliance along the piezo-active coordinate. Thus, a large compliance plus a large dipole moment derivative can be achieved simultaneously, leading to a large piezo-coefficient. Molecules of the molecular spring type thus seem particularly attractive to explore for improved piezo-materials.

In short, electromechanical hydrogen bonds and molecular systems are likely to be ubiquitous and can be rapidly screened using accurate first-principles electronic structure calculations. On the basis of the trade-off between hydrogen bond strength and change in dipole moment in intermolecular interactions, we believe that electric-field driven molecular conformational changes will bring more substantial piezoelectric response and that deformable hydrogen bonds can be used to produce polar, self-assembled piezoelectric materials designed through computational approaches.

■ COMPUTATIONAL DETAILS

We now review the process of calculating the piezo-coefficient, which is similar to our earlier approach.[1] We first generated the dimer molecules from our database in Avogadro.[27] For all calculations we used the B3LYP density functional[28,29] in combination with the 6-31G* basis,[30,31] which we found to qualitatively reproduce higher-level results.[1] A development version of the Q-Chem program package was used throughout.[32] After the dimer geometries were optimized at zero field, the hydrogen bonds were aligned along the z-axis, so the piezo-response could be investigated by potential energy surface scans along the z-axis. We then performed subsequent calculations on the dimer pairs at varying field strengths applied along the z-axis (cf. Figure 1). The field strengths typically ranged between −1.0 and 1.0 V/nm, incremented in steps of 0.25 V/nm.

dx.doi.org/10.1021/jp412740j | J. Phys. Chem. A 2014, 118, 7404−7410

For each field strength, we scanned the potential energy surface by varying the dimer distances, z, in steps of about 0.02 Å and calculated single-point energies at each point. We plotted the energy versus hydrogen bond distance and performed a polynomial fit (usually of order 6) of the data. The equilibrium (minimum energy) hydrogen bond length for each field was found from the fit and was used to determine the piezo-coefficient. It is worthwhile to mention that the minimum energy hydrogen bond length could also be found via geometry optimizations of the dimers subjected to external fields, but as shown previously,[1] this involves complications in maintaining the hydrogen-bond geometry and can be time-consuming. Furthermore, the constraints implicit to the scanning method were shown to yield similar results to the optimization method.[1] To this end, we plotted the equilibrium bond lengths versus the field strength for each dimer pair. The slope of a linear regression performed for the data of one of these plots can then be used to calculate the piezo-coefficient:

$$d_{33} \approx \frac{1}{z_0} \times \text{slope} \tag{16}$$

It should be noted that for one dimer (molecule **2a**), the equilibrium distance vs field strength plot showed strong nonlinearity above 0.5 V/nm field strength. For this compound, these three points were deleted and the linear regression was performed as usual (see Supporting Information). This is a potential problem in this finite-field approach but is avoided in the new method of piezocoefficient determination, which utilizes eq 1. Looking more closely at eq 15, the degree of nonlinearity will likely depend on the displacement derivative of the polarizability for the molecule. Examples of the data analysis procedure are given in the Supporting Information.

An intuitive interpretation for eq 16 is that the slope is related to dz_{min}/df, where z_{min} is the equilibrium hydrogen bond length at field strength f. The piezo-coefficient can be defined as dS_z/df, where S_z is the strain in the z direction for the system. The strain can be viewed as the fraction or percent deformation in the z direction, which one can approximate as dz_{min}/z_0, and dividing this term by df yields eq 16.

The method just described for piezo-coefficient calculation typically requires many single-point energy calculations in addition to an initial geometry optimization. For example, in this study, after the initial geometry optimization was performed, typically around 99 single-point energy calculations were carried out (for each of the 9 field strengths, typically 11 single-point energies were calculated to scan the potential energy surface). Given eq 1, we can in practice reduce the number of single-point energy calculations by an order of magnitude.

We now outline how we estimate the piezo-coefficient for our systems based on eq 1. z_0 was determined in the zero-field geometry optimization. Furthermore, the Hessian $h_{0\xi\xi} \equiv (\partial^2 E/\partial\xi^2)|_{(z0,0)}$ was obtained from scanning the potential energy surface at zero field, which requires only on the order of 11 single-point calculations, and performing a polynomial fit of the data as described above. From the fit equation and the equilibrium hydrogen bond length, it is then straightforward to determine $h_{0\xi\xi}$.

No additional calculations are typically necessary to determine $\mu_{0\xi} \equiv (\partial^2 E/\partial f\partial\xi)|_{(z0,0)}$ since the potential energy surface has already been scanned and the dipole moments can be collected from the previous calculations. The derivative is evaluated numerically from the z-component of the dipole moment for the two single point energy calculations for the two single-point energy calculations closest to the equilibrium hydrogen bond length:

$$\mu_{0\xi} \approx \frac{\mu(z_2) - \mu(z_1)}{z_2 - z_1} \tag{17}$$

Here, z_1 and z_2 are the hydrogen bond lengths nearest to the equilibrium bond length. The inverse Hessian and dipole moment derivatives were then combined to estimate the piezo-coefficient according to eq 1.

At this point, it should be noted that the dipole derivatives calculated here numerically introduce some unknown error into our approximation of the piezo-coefficient. It is therefore advisable to choose appropriate displacements in the separation coordinate z in order to evaluate the piezo-coefficient with reasonable accuracy. There are also well-known methods for efficiently and accurately calculating diopole derivatives, which involve the numerical calculation of the field-derivative of the gradient.[33] Euler's relation, which is actually also used in the derivation section, allows us to write $(\partial^2 E/\partial\xi\partial f) \equiv (\partial^2 E/\partial f\partial\xi)$ or $\partial\mu/\partial\xi \equiv \partial g/\partial f$, where g is of course the gradient.

For the determination of hydrogen bond energies within our system database, we simply used the difference in energy between the optimized isolated monomers and the dimers. We are aware that the energies are very approximate without counterpoise correction or dispersion correction, but here we aim only at the investigation of qualitative trends.

■ ASSOCIATED CONTENT

Supporting Information

Equilibrium structures, samples for data analysis, and raw data for system **2a**. This material is available free of charge via the Internet at http://pubs.acs.org.

■ AUTHOR INFORMATION

Corresponding Author

*(D.S.L.) E-mail: qclab@pitt.edu. Phone: 412-624-8912. Fax: 412-624-8301.

Notes

The authors declare no competing financial interest.

■ ACKNOWLEDGMENTS

The authors thank Adam Gagorik for useful discussions and help with Python implementations. K.A.W. acknowledges an Arts & Sciences graduate student fellowship from the University of Pittsburgh. D.S.L. acknowledges start-up funding from the University of Pittsburgh as well as computer time at the Center for Simulation and Modeling at the University of Pittsburgh. G.R.H. thanks AFOSR (FA9550-12-1-0228) for support.

■ DEDICATION

Dedicated to Professor Kenneth Jordan on the occasion of his 65th birthday.

■ REFERENCES

(1) Werling, K. A.; Hutchison, G. R.; Lambrecht, D. S. Piezoelectric effects of applied electric fields on hydrogen-bond interactions: First-principles electronic structure investigation of weak electrostatic interactions. *J. Phys. Chem. Lett.* **2013**, *4*, 1365−1370.

(2) Quan, X.; Marvin, C. W.; Seebald, L.; Hutchison, G. R. Single-molecule piezoelectric deformation: Rational design from first-principals calculations. *J. Phys. Chem. C* **2013**, *117*, 16783−16790.
(3) Cohen, R. E. *Piezoelectricity*; Springer Berlin Heidelberg: Berlin, Germany, 2008; pp 471−492.
(4) Vanderbilt, D. First-principles based modelling of ferroelectrics. *Curr. Opin. Solid State Mater. Sci.* **1997**, *2*, 701−705.
(5) Fu, H.; Cohen, R. Polarization rotation mechanism for ultrahigh electromechanical response in single-crystal piezoelectrics. *Nature* **2000**, *403*, 281−283.
(6) Fu, H.; Bellaiche, L. First-principles determination of electromechanical responses of solids under finite electric fields. *Phys. Rev. Lett.* **2003**, *91*, 057601.
(7) Bester, G.; Wu, X.; Vanderbilt, D.; Zunger, A. Importance of second-order piezoelectric effects in zinc-blende semiconductors. *Phys. Rev. Lett.* **2006**, *96*, 187602.
(8) Armiento, R.; Kozinsky, B.; Fornari, M.; Ceder, G. Screening for high-performance piezoelectrics using high-throughput density functional theory. *Phys. Rev. B* **2011**, *84*, 014103.
(9) Bystrov, V. S.; Paramonova, E. V.; Bdikin, I. K.; Bystrova, A. V.; Pullar, R. C.; Kholkin, A. L. Molecular modeling of the piezoelectric effect in the ferroelectric polymer poly(vinylidene fluoride) (PVDF). *J. Mol. Model.* **2013**, *19*, 3591−3602.
(10) Avanci, L. H.; Cardoso, L. P.; Girdwood, S. E.; Pugh, D.; Sherwood, J. N.; Roberts, K. J. Piezoelectric coefficients of mNA organic nonlinear optical material using synchrotron X-ray multiple diffraction. *Phys. Rev. Lett.* **1998**, *81*, 5426−5429.
(11) Bain, A. M.; El-Korashy, N.; Gilmour, S.; Pethrick, R. A.; Sherwood, J. N. Ultrasonic and piezoelectric investigations on single crystals of 3-nitroaniline. *Philos. Mag. B* **1992**, *66*, 293−305.
(12) Paturle, A.; Graafsma, H.; Sheu, H.-S.; Coppens, P.; Becker, P. Measurement of the piezoelectric tensor of an organic crystal by the X-ray method: The nonlinear optical crystal 2-methyl 4-nitroaniline. *Phys. Rev. B* **1991**, *43*, 14683−14691.
(13) Lipscomb, G. F.; Garito, A. F.; Narang, R. S. An exceptionally large linear electro-optic effect in the organic solid MNA. *J. Chem. Phys.* **1981**, *75*, 1509−1516.
(14) Kerkoc, P.; Maruo, S.; Horinouchi, S.; Sasaki, K. Piezoelectric and electro-optic coefficients of the molecular nonlinear optical crystal 2-furyl methacrylic anhydride. *Appl. Phys. Lett.* **1999**, *74*, 3105−3106.
(15) DiBenedetto, S. A.; Frattarelli, D.; Ratner, M. A.; Facchetti, A.; Marks, T. J. Vapor phase self-assembly of molecular gate dielectrics for thin film transistors. *J. Am. Chem. Soc.* **2008**, *130*, 7528−7529.
(16) Facchetti, A.; Annoni, E.; Beverina, L.; Morone, M.; Zhu, P.; Marks, T. J.; Pagani, G. A. Very large electro-optic responses in H-bonded heteroaromatic films grown by physical vapour deposition. *Nat. Mater.* **2004**, *3*, 910−917.
(17) Frattarelli, D.; Schiavo, M.; Facchetti, A.; Ratner, M. A.; Marks, T. J. Self-assembly from the gas-phase: design and implementation of small-molecule chromophore precursors with large nonlinear optical responses. *J. Am. Chem. Soc.* **2009**, *131*, 12595−12612.
(18) Johal, M. S.; Cao, Y. W.; Chai, X. D.; Smilowitz, L. B.; Robinson, J. M.; Li, T. J.; McBranch, D.; Li, D. Spontaneously self-assembled polar asymmetric multilayers formed by complementary H-bonds. *Chem. Mater.* **1999**, *11*, 1962−1965.
(19) Ward, M. D.; Raithby, P. R. Functional behaviour from controlled self-assembly: challenges and prospects. *Chem. Soc. Rev.* **2013**, *42*, 1619−1636.
(20) Zhu, P.; Kang, H.; Facchetti, A.; Evmenenko, G.; Dutta, P.; Marks, T. J. Vapor phase self-assembly of electrooptic thin films via triple hydrogen bonds. *J. Am. Chem. Soc.* **2003**, *125*, 11496−11497.
(21) Munn, R. W. Theory of piezoelectricity, electrostriction, and pyroelectricity in molecular crystals. *J. Chem. Phys.* **2010**, *132*, 104512.
(22) Gale, J. D. GULP: A computer program for the symmetry-adapted simulation of solids. *J. Chem. Soc., Faraday Trans.* **1997**, *93*, 629−637.
(23) Gale, J. D.; Rohl, A. L. The General Utility Lattice Program (GULP). *Mol. Simul.* **2003**, *29*, 291−341.
(24) Clark, R.; Romero, A.; Borbulevych, O.; Antipin, M.; Nesterov, V.; Timofeeva, T. 2-Amino derivatives of 5-nitrophenylacetamide. *Acta Crystallogr., Sect. C: Cryst. Struct. Commun.* **2000**, *56* (Pt 3), 336−338.
(25) Seidler, T.; Stadnicka, K.; Champagne, B. In *SPIE Organic Photonics + Electronics*; Eich, M., Nunzi, J.-M., Jakubiak, R., Eds.; SPIE: Bellingham WA, 2013; p 88270Y.
(26) Greeley, J.; Stephens, I. E. L.; Bondarenko, A. S.; Johansson, T. P.; Hansen, H. A.; Jaramillo, T. F.; Rossmeisl, J.; Chorkendorff, I.; Norskov, J. K. Alloys of platinum and early transition metals as oxygen reduction electrocatalysts. *Nat. Chem.* **2009**, *1*, 552−556.
(27) Hanwell, M. D.; Curtis, D. E.; Lonie, D. C.; Vandermeersch, T.; Zurek, E.; Hutchison, G. R. Avogadro: An advanced semantic chemical editor, visualization, and analysis platform. *J. Cheminf.* **2012**, *4*, 17.
(28) Becke, A. D. Density-functional thermochemistry. III. The role of exact exchange. *J. Chem. Phys.* **1993**, *98*, 5648.
(29) Lee, C.; Yang, W.; Parr, R. Development of the Colle−Salvetti correlation-energy formula into a functional of the electron density. *Phys. Rev. B: Condens. Matter* **1988**, *37*, 785−789.
(30) Hehre, W. J. Self-consistent molecular orbital methods. XII. Further extensions of gaussian-type basis sets for use in molecular orbital studies of organic molecules. *J. Chem. Phys.* **1972**, *56*, 2257.
(31) Hariharan, P. C.; Pople, J. A. The effect of d-functions on molecular orbital energies for hydrocarbons. *Chem. Phys. Lett.* **1972**, *16*, 217−219.
(32) Shao, Y.; et al. Advances in methods and algorithms in a modern quantum chemistry program package. *Phys. Chem. Chem. Phys.* **2006**, *8*, 3172−3191.
(33) Komornicki, A.; McIver, J. W. An efficient abinitio method for computing infrared and Raman intensities: Application to ethylene. *J. Chem. Phys.* **1979**, *70*, 2014−2016.